ELSEVIER

A study of zircon crystallization, structure, and chemical resistance relationships in ZrO$_2$ containing ceramic glazes

Irina Atkinson*, Oana C. Mocioiu, Elena M. Anghel

Institute of Physical Chemistry "Ilie Murgulescu" of the Romanian Academy, 202 Splaiul Independentei, 060021 Bucharest, Romania

ABSTRACT

This study aims to investigate zircon (ZrSiO$_4$) formation during thermal treatment and its influence on the structure and properties of the ceramic glazes. Four raw ceramic glazes with the addition of 5, 9, 13, and 17 wt% of ZrO$_2$ (<5 μm) at the expense of SiO$_2$ were prepared by the ceramic traditional route. To obtain homogeneous melting and consequently a high-quality surface, 5 wt% of colemanite (2CaO·3B$_2$O$_3$·5H$_2$O) was added to the ceramic glazes formulation. XRD, NMR, Raman spectroscopy and FTIR measurements revealed the formation of ZrSiO$_4$. An increase of ZrSiO$_4$ from 35 to 86 wt% with an increase of ZrO$_2$ content in the composition of ceramic glazes was observed. ^{29}Si solid-state MAS NMR measurements also showed that with successive increases of ZrO$_2$ concentration the relative intensity of zircon resonance increases. The evaluation of the chemical resistance revealed the beneficial effect of ZrSiO$_4$ on this property.

Un estudio de cristalización de circón, relaciones de estructura y resistencia química en esmaltes cerámicos que contienen ZrO$_2$

RESUMEN

Este estudio examina la formación de circón (ZrSiO$_4$) durante el tratamiento térmico y su influencia en la estructura y propiedades de los esmaltes cerámicos. Cuatro esmaltes cerámicos fueron preparados con la adición de 5, 9, 13 y 17% en peso de ZrO$_2$ (<5 μm) a expensas de SiO$_2$ utilizando técnicas tradicionales. Para obtener una fusión homogénea y, en consecuencia, una superficie de alta calidad, se añadió un 5% en peso de colemanita (2CaO-3B$_2$O$_3$-5H$_2$O) a la formulación de los esmaltes cerámicos. Las mediciones de XRD, NMR, espectroscopia Raman y FTIR revelaron la formación de ZrSiO$_4$. Se observó un aumento de ZrSiO$_4$ del 35 al 86% en peso con un aumento del contenido de ZrO$_2$ en la composición de los esmaltes cerámicos. Las mediciones de NMR del ^{29}Si estado sólido también mostraron que

---

* Corresponding author.
  E-mail address: irinaatkinson@yahoo.com (I. Atkinson).

con los incrementos sucesivos de la concentración de ZrO_2 aumenta la intensidad relativa de la resonancia del circón. La evaluación de la resistencia química reveló el efecto beneficioso del $ZrSiO_4$ sobre esta propiedad.

Introduction

Ceramic glazes are used to form a layer over a ceramic body and are prepared from a mixture of natural minerals. They play an important role in the esthetical aspect and durability of the final ceramic products [1,2]. Generally, the ceramic glazes are constituted of an amorphous phase and one or more crystalline phases [3–5]. The chemical composition of the glazes and their thermal treatment cycle from the sintering temperature to cooling plays an important role on ceramic glaze crystallization.

Both they determine the final phase composition of the glass-ceramics, the quantity of the crystalline phase, and properties of the final materials; surface smoothness, gloss, color, thermal expansion coefficient, wear-resistance and also chemical durability [2].

For corrosive solutions, chemical durability is an important factor in assessing a glaze lifetime duration, and it is a key reason for applying ceramic glazes on ceramic products. Chemical stability has been frequently reported in terms of the corrosion of the glassy phase in various pH environments and to a lesser extent to the crystalline phases, stresses, and chemical gradients at crystal-glass boundary [4]. Thus, lowering the content of alkali and high alumina additions improves the glassy phase durability. It is known that zircon [6] highly influences the surface properties of ceramic glazes [7] as well as the main crystalline phases developed in ceramic glazes (mullite, $Al_2Si_2O_{13}$, anorthite, $CaAl_2Si_2O_8$, and wollastonite, $CaSiO_3$).

Zircon is used in the composition of ceramic glazes due to its performance such as increase opacity and brightness, thermal stability, good resistance to chemical attack, and high wear resistance [6,8]. To promote in situ zircon crystallization monoclinic zirconia can be used in ceramic glaze formulations as a nucleation agent [5].

As was aforementioned, the thermal treatment cycle plays an important role in the final properties of the ceramic product and cost. Conventionally ceramic glazes are obtained from glaze compositions prepared with frits that increase considerably the energy cost.

Nowadays, researchers have focused on finding alternatives to lower the synthesis temperature and eliminate the glaze melt fritting process resulting in the reduction of energy consumption during the manufacturing process [9–11]. In contrast to fritted glaze compositions, raw ceramic glazes are cost-effective and less time-consuming replacements for application to ceramic substrates.

In the current work, in order to obtain a homogeneous melting and improved properties of the ceramic glazes, 5 wt% of colemanite was added in the ceramic glazes formulation. Colemanite is a natural source of insoluble boron that can be considered an alternative to boron precursor in raw ceramic glaze since it has the glass-forming ability and reduces the melting point, provides homogeneous melting and stable structure, and positively influence the chemical and physical properties of the final ceramic product [10]. Not many research studies exist related to the use of colemanite as a boron precursor in raw ceramic glazes [9]. Its addition (3 wt%) to the hard porcelain formulations resulted in a decrease of firing temperature and reduction of porosity and water absorption as was reported by S. Akpinar et al. [10].

This work aimed to understand the influence of compositional variation on the type of crystalline phases formed (with emphasis on zircon) during thermal treatment and their effect on the structure and chemical durability of the ZrO_2 containing ceramic glazes.

Experimental

Ceramic glaze preparation

In the present study, four raw ceramic glazes with the addition of 5, 9, 13, and 17 wt% respectively of ZrO_2 at the expense of SiO_2 (Table 1) were prepared by ceramic traditional route. The starting materials were feldspar ($KAlSi_3O_8$), quartz (SiO_2), kaolin ($Al_2Si_2O_5(OH)_4$), wollastonite ($CaSiO_3$), zinc oxide (ZnO), colemanite ($2CaO–3B_2O_3–5H_2O$) (industrial grade-Clayman Supplies-UK), and ZrO_2 (Sigma Aldrich). The detailed synthesis procedure has been described in our previous works [12,13]. In brief, the raw materials were wet milled (balls: material: water ratio of 1.5:1:0.6) up to 0.1% residue on a sieve of 63 μm. The resulted slurry was applied on the unfired ceramic substrate followed by thermal treatment with a ramp rate of 10 °C/min up to 1250 °C for 1 h plateau in an electrical furnace. The obtained samples were labeled as following: G5Z, G9Z, G13Z, and G17Z. The theoretical oxide composition of ceramic glazes expressed in weight % is presented in Table 1.

Characterization methods

XRD patterns were collected using a Rigaku UltimaIV diffractometer (Cu Kα radiation, $\lambda = 1.5406$ Å) operating at 40 kV and 30 mA, in the range of 10–80° with a step size of 0.02 and a speed of 2°/min. Qualitative and quantitative phase analyses were performed using Rigaku's PDXL software, connected to ICDD PDF-2 database. The XRD patterns of the obtained ceramic glazes were refined by the whole Pattern Powder Fitting (WPPF) method using the split-pseudo Voigt function and the B-spline background model. The following parameters confirm the fitting quality of the experimental data: the goodness of fit S that should be closed to 1 for a good fit and,

Table 1 – Theoretical chemical composition of the studied glazes (wt%).								
Sample	Na₂O	K₂O	CaO	ZnO	Al₂O₃	SiO₂	ZrO₂	B₂O₃
G5Z	1.56	3.31	9.72	1.43	11.55	64.79	5	2.64
G9Z	1.49	3.18	9.33	1.37	11.08	62.03	9	2.53
G13Z	1.42	3.02	8.82	1.30	10.49	59.62	13	2.42
G17Z	1.36	2.90	8.51	1.24	10.10	56.58	17	2.31

Rwp (weighted differences between measured and calculated values) that should close to or less than 10%.

The microstructure of the samples was analyzed using a Zeiss SUPRA 55VP Scanning Electron Microscope equipped with energy dispersive X-ray analysis (EDX) capability.

The ^{29}Si solid-state MAS NMR spectra were recorded using a Varian Infinity Plus spectrometer with a 7.05 T magnet at a Larmor frequency of 59.6 MHz. The powder samples were packed into 7 mm zirconia rotors and spun at 4 kHz. All collected spectra were referenced to tetramethylsilane at 0 ppm. Simulations using four and five Gaussian peaks were carried out using the Dmfit software [14].

^{27}Al solid state MAS NMR spectra were acquired at MAS frequency of 18 kHz on a Bruker Advance II+ spectrometer equipped with a magnet of 14.1 T (Larmor frequency of 156.37 MHz). The powder samples were packed into 3.2 mm zirconia and $Y_3Al_5O_{12}$ was used as a reference with the AlO_6 resonance set to 0.7 ppm.

Micro-Raman data were measured by means of a LabRam HR800 spectrometer from Jobin–Yvon–Horiba, equipped with a 532 nm laser line and a grating of 1800 lines. The backscattered light was collected through the 50x LWD/0.55 objective (~1.18 μm spot size) of an Olympus microscope. To improve sensitivity in detecting surface structure of the glazes under investigation, UV-Raman spectra were collected by a 325 nm laser line, through a 40×/0.47 NUV objective, from a sample spot size less than 1 μm. Grating of 2400 lines was used in the latter configuration. Edge filter prevent us recording UV-Raman spectra at low wavenumbers.

Infrared transmission spectra were recorded using Nicolet 6700 spectrophotometer in the 400–1400 cm^{-1} range. The same weight of the ceramic glaze powder was dispersed in KBr pellet.

The chemical resistance of the prepared ceramic glazes was evaluated based on DIN 12116 for acid resistance and ISO 695 for alkali resistance respectively. In brief for acid resistance evaluation, the glaze surface to be tested is boiled for 6 h in 20% hydrochloric acid [c (HCl) = 6 mol/l], and the weight loss is determined in mg/100 cm^2. In the case of alkali resistance assessment (ISO 695), glaze surface is subjected to a 3 h treatment in a boiling aqueous solution consisting of equal volumes of sodium hydroxide, c (NaOH) = 1 mol/l and sodium carbonate, c(Na₂CO₃) = 0.5 mol/l.

Results and discussion

X-ray diffraction XRD

X-ray analysis of the prepared ceramic glazes was carried out to assess the crystallization of zircon. Fig. 1 shows the XRD patterns corresponding to ceramic glazes after thermal treatment at 1250 °C. In all investigated glazes, the formation of zircon-ZrSiO₄ (JCPDS card no. 00-006-0266) as a major phase occurs.
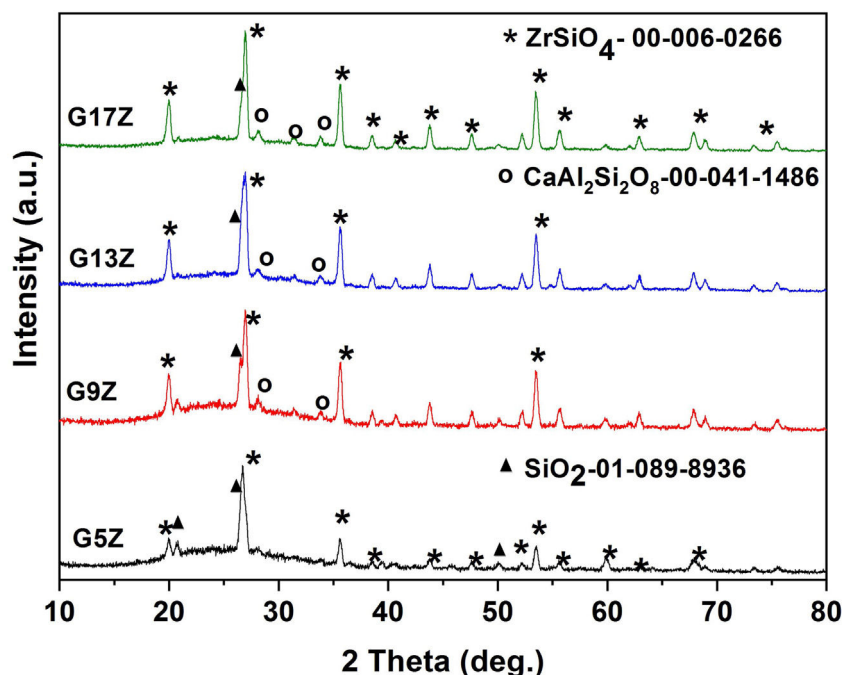

Fig. 1 – XRD patterns of the studied ceramic glazes.

Table 2 – XRD data analysis.

Sample	Phase name	Content (wt%)	Crystallinity (%)	Fitting parameters	
				Rwp	S
G5Z	Zircon	35	29	8.98	1.031
	Anorthite	7			
	Quartz	58			
G9Z	Zircon	49	42	8.59	1.003
	Anorthite	20			
	Quartz	31			
G13Z	Zircon	57	53	8.78	1.044
	Anorthite	28			
	Quartz	15			
G17Z	Zircon	86	87	11.28	1.146
	Anorthite	8			
	Quartz	5			

In addition, anorthite-$CaAl_2Si_2O_8$ (JCPDS card no.00-041-1486) and quartz-SiO_2 (JCPDS card no. 01-0850794) were also identified beside the amorphous halo between 2theta 20–35°. As can be observed from Table 2 the amount of zircon continuously increases, from 35 wt% (G3Z) to 86 wt% (G17Z) with the increase of ZrO_2 concentration. A similar trend was also observed for the glaze degree of crystallinity. A crystallinity of 87% was determined for the glaze with the highest ZrO_2 content (17 wt%).

MAS NMR spectra

^{29}Si MAS NMR

^{29}Si solid-state MAS NMR is a useful method for determining the state of silicon polymerization. The ^{29}Si chemical shifts for SiO_4 (Q^4) units range from 60 to 110 ppm. The silicon environment in aluminosilicates can be designated as Qn(mAl), where n denotes the number of bridging oxygen (BO) for each Q unit and m represents the number of attached AlO_4 ($m \leq n$). The substitution by Al of each of the four silicons surrounding the central Si determines the displacement of the chemical shift of about 5 ppm toward less negative values.

All the studied ceramic glazes exhibit broad featureless spectra indicating a disordered structure (Fig. 2). The deconvolution of the ^{29}Si MAS NMR spectra (Table 3) yielded resonances at approx. −105, −98, 89 and −81 ppm. In the case of G13Z ceramic glazes an additional peak resonance at −76 ppm that represents the Q^1 site of silicon environment, was observed. The peaks located at −105, −98, and −89 ppm are assigned to Q^4(1Al), Q^4(2Al), and Q^4(3Al) units while the narrow peak at −81 ppm corresponding to zircon. I. Farnan and E.K.H. Salje reported [15] that crystalline undamaged zircon shows a single sharp ^{29}Si NMR resonance at a chemical shift of −81.5 ppm. Quantification of the relative intensity
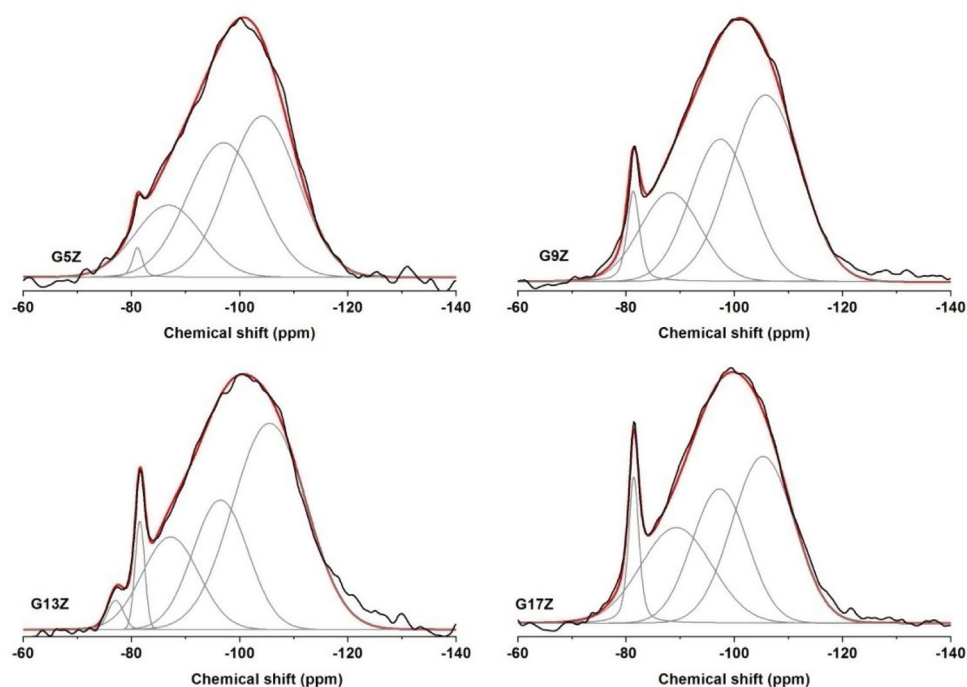

Fig. 2 – ^{29}Si MAS NMR spectra of the studied ceramic glazes.

Table 3 – Solid state ^{29}Si MAS NMR data.															
Sample	Q^4(1Al)			Q^4(2Al)			Q^4(3Al)			ZrSiO$_4$			Q1		
	δ	Δ	%	δ	Δ	%	δ	Δ	%	δ	Δ	%	δ	Δ	%
G5Z	−104	1.5	43.26	−97	1.4	37.12	−87	18.25	1.2	−81	0.2	1.37	–	–	–
G9Z	−105	1.5	45.84	−98	1.3	27.29	−89	23.92	1.3	−81	0.2	2.95	–	–	–
G13Z	−105	1.6	52.04	−97	1.2	24.42	−87	18.63	1.3	−82	0.2	3.47	−76	0.3	1.44
G17Z	−105	1.4	39.06	−97	1.2	28.18	−89	25.66	1.5	−81	0.2	7.10	–	–	–

δ – chemical shift, ±1 ppm; Δ – peak width, ±0.5 kHz; % – integrated intensity, ±2.

of zircon resonance in the ^{29}Si MAS NMR spectra of ceramic glazes increases from 1.37% for G5Z sample to 7.10% for G17Z sample with the highest content of zircon as was revealed by XRD measurements.

As can be noticed from ^{29}Si MAS NMR results the quartz determined by XRD measurements could not be identified by NMR probably due to the much longer T1 relaxation time observed in crystalline systems mostly for spin-1/2 nuclei such as ^{29}Si [16].

^{27}Al MAS NMR

^{27}Al solid-state MAS NMR spectra of the studied ceramic glazes are presented in Fig. 3 and the deconvolution results are listed in Table 4. The FWHM of the ^{27}Al MAS NMR resonance is not reported, due to the second-order quadrupolar peak broadening of this nucleus [16]. The ^{27}Al MAS NMR spectra of ceramic glazes display two resonances at ca. 54 ppm and 13 ppm respectively. The first resonance corresponds to AlO$_4$ (over 90%) suggesting that aluminum acts mainly as a network former in the ceramic glazes under investigation. A small quantity of AlO$_6$ form, indicating that to some extend aluminum acts a network modifier as well, was also identified. This finding is well correlated with the structural role of aluminum and its intermediate behavior. When Al acts as a network former, the equilibrium of electric charge, is usually achieved by charge compensating alkali or alkaline-earth cations (one Me$^+$ ion in a neighbor of one AlO$_4$$^-$, one

Me^{2+} ion in a neighbor of two AlO$_4$$^-$ or one non-bridging oxygen NBO as well as one AlO$_4$$^-$). If such ions are not available for charge compensating the neutrality of negatively charged AlO$_4$$^-$ tetrahedra is achieved by changing Al coordination to a higher number that assumes a positive charge. Non-framework alkali or alkaline-earth cations can act as either charge-balancing or network modifying cations depending on composition leading to the formation of NBO and as a result decreases the degree of polymerization.

Raman spectroscopy

Raman spectroscopy has enabled structural investigation of both crystalline and vitreous phases present in silicate glass-ceramics.

Spectral features of zircon, ZrSiO$_4$, at 1009 cm^{-1} (ν_3 modes of SiO$_4$ with B$_{1g}$ symmetry), 975 cm^{-1} (ν_1 modes with A$_{1g}$ symmetry), 440 cm^{-1} (ν_2 symmetric bending in isolated SiO$_4$, Q$^\circ$, with A$_{1g}$ symmetry) and 269 cm^{-1} (B$_{2g}$, ν_2 bending) and less intense external modes (356, 224 and 202 cm^{-1}) [17,18] prevail in the Raman spectrum of G17Z in Fig. 4. More intense zircon spectral features are present in the UV-Raman spectra of the G (5/9/13/17) Z glazes either due to higher zircon content at the surface and/or resonant Raman effect (see inset of the Fig. 4). Lowering of the zircon symmetry in the G13Z spectrum caused shifting of the ν_1 and ν_3 modes toward lower wavenumbers (inset of the Fig. 4). Moreover, G17Z glaze contains both zircon and lowered symmetry zircon (the 1009 cm^{-1} band and its shoulder at 1003 cm^{-1}). Lack of the doublet at ~179/191 cm^{-1} invalidates formation of monoclinic zirconia [19] in case of G17Z. Much wider and less intense peaks at 142, 266 and 478 cm^{-1} (shoulder of the 467 cm^{-1} peak) might originate from amorphous zirconia [19]. Presence of α-quartz in the G17Z might be signaled by the peak at 467 cm^{-1} [20].

Despite low content of the B$_2$O$_3$ in the G (5/9/13/17) Z glazes, tinny bands at 1321 and 1466 cm^{-1} might belong to BØ$_2$O$^-$ linked to AlØ$_4$$^-$ in aluminum metaborates (Ø is bridging oxygen) and B—O stretching mode in (BO$_3$)$^-$ metaborate rings and/or chains, respectively [21,23]. Wide peaks at 822, 871, 1059, 1089 and 1185 cm^{-1} are attributable to symmetric Si—O stretching of the Q^0, Q^3 and Q^4 units (0, 3 and 4 stand for number of bridging oxygen per SiO$_4$ tetrahedra) in silicate glasses [22–24]. The other two regions of the Raman spectra of the silicate glasses, e.g. <400 cm^{-1} due to lattice modes and network modifying cations as well as 400–800 cm^{-1} range originating from Si—O—Si bending modes among SiO$_4$ tetrahedra [25], are rather overwhelmed by the strong zircon modes (Fig. 5).
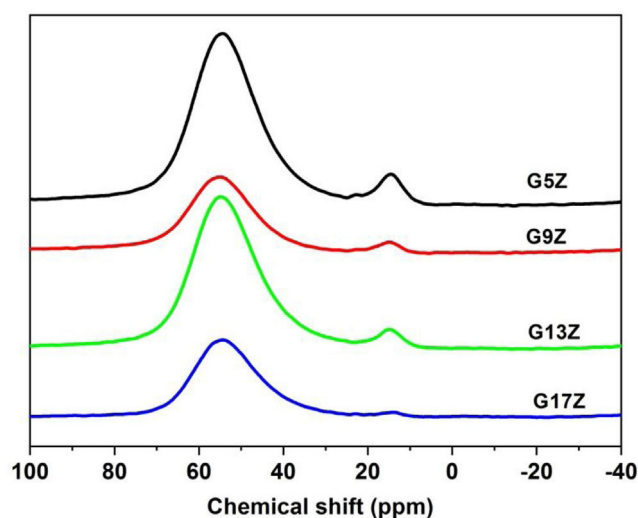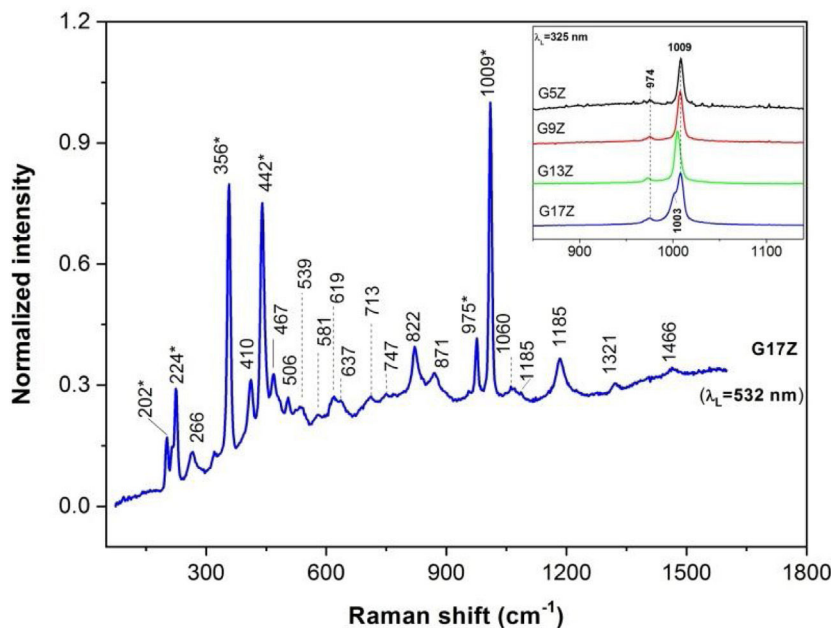

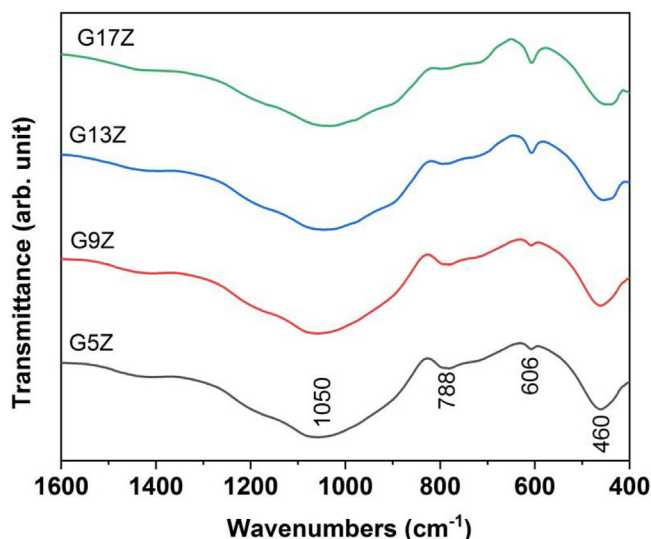Fig. 3 – ^{27}Al MAS NMR spectra of the studied ceramic glazes.

Table 4 – Solid state ^{27}Al MAS NMR data.

Sample	AlO$_4$		AlO$_6$	
	$\delta \pm 1$ (ppm)	$\% \pm 2$	$\delta \pm 1$ (ppm)	$\% \pm 2$
G5Z	53	91.58	13	8.41
G9Z	54	94.29	15	5.71
G13Z	54	96.46	15	3.54
G17Z	54	98.62	14	1.38

Fig. 4 – Raman spectrum of G17Z ceramic glaze (* stands for zircon vibration modes). Inset represents UV-Raman spectra of the G(5/9/13/17)Z ceramic glazes over 850–1140 cm^{-1} range.

IR spectroscopy

FTIR spectra displayed in Fig. 5 reveal the presence of three vibration bands corresponding to Si—O—Si bonds: the broad one at 1050 cm^{-1} (asymmetric stretching vibration), at 788 cm^{-1} (symmetric stretching vibration) and 460 cm^{-1} (bending vibrations) respectively [26]. The displacement of the first two bands regarding to those of silica (1080 and 800 cm^{-1}) is due to the presence of network modifiers (K$_2$O, Na$_2$O, CaO, ZnO) in ceramic glazes formulation. Along with the vibration bands related to the silica network, a vibration band at 606 cm^{-1} attributed to Si—O—Zr bond of ZrSiO$_4$ was also noticed [27]. An increase of the band intensity located at 606 cm^{-1} with the increasing amount of formed zircon was observed.

SEM

SEM investigations of the G5Z and G17Z ceramic glazes are shown in Figs. 6 and 7. The microstructure of the glaze surface is quite heterogeneous consisting of crystalline phases and residual glassy matrix which appears in dark contrast. The EDX analysis of the glassy matrix (Fig. 7b) exhibited the presence of silicon, aluminum and oxygen as predominant constituents. The white crystals are assigned to ZrSiO$_4$ as a result of zirconia reaction with silica while the darker crystals (indicate by the circle in Fig. 7a) seem to correspond to quartz as was revealed by EDX element map (Fig. 7b) and in good agreement with XRD results. Si accumulation constitutes

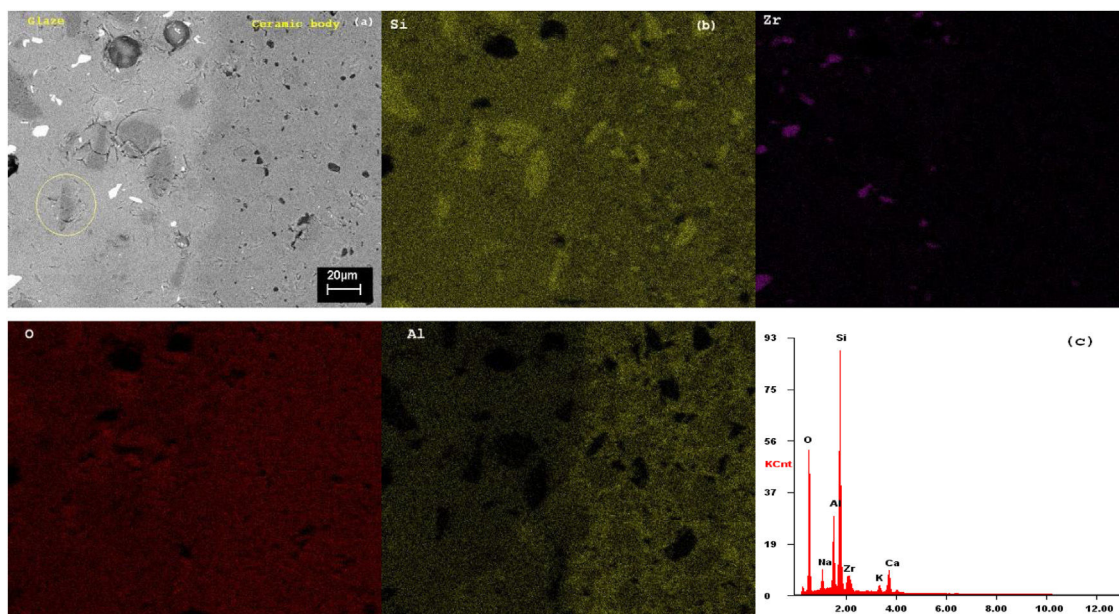**Fig. 5 – FTIR spectra of the studied ceramic glazes.**

Fig. 6 – SEM image of the glaze ceramic/substrate interface for G5Z sample (a) EDX mapping for Zr, Si, Al, and O (b) and EDX analysis of the surface of ceramic glaze (c).
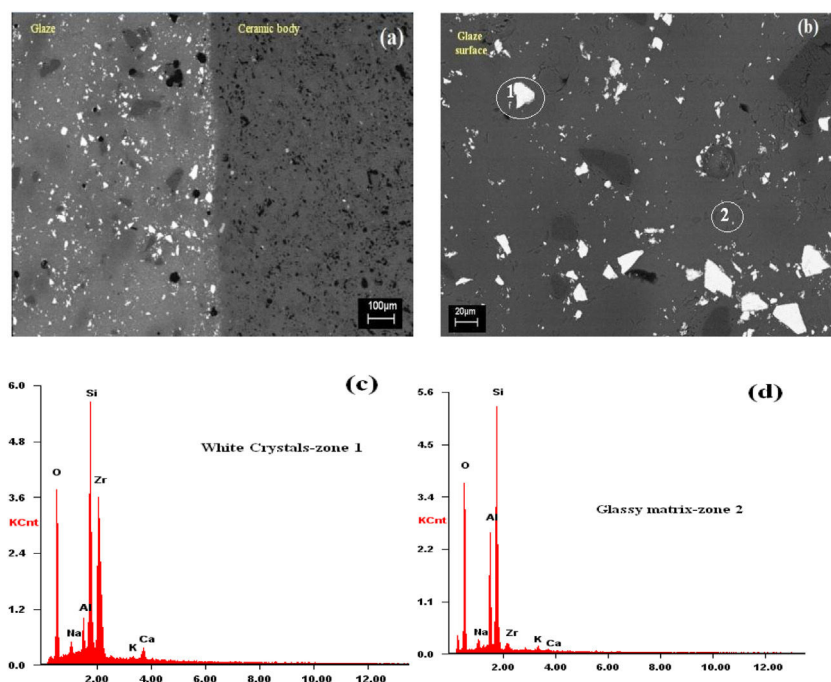

Fig. 7 – SEM images of the glaze–ceramic substrate interface for G17Z sample (a) glaze surface (b) and the EDX analyses of the white crystals (c) and, glassy matrix (d).

a part of the ceramic body as well as the glaze. The white crystals are all enriched in Zr indicating the formation of zircon. Moreover, the EDX spectra of the surface of ceramic glazes (Figs. 6c and 7c) confirm also zircon crystallization.

Chemical durability

The chemical durability of the prepared ceramic glazes in acidic and alkaline solutions was determined according to DIN 12116 and ISO 695 respectively. The obtained results are presented in Table 5. As can be observed, a very good chemical resistance against the hydrochloric acid solution was obtained for G13Z and G17Z ceramic glazes with the highest zircon content and degree of crystallinity. In contrast, the G5Z and G9Z ceramic glazes with lower content of $ZrSiO_4$ received chemical acid resistance classification (class 2). Standard DIN 12116 divides glass types into four classes. If half the weight loss of the surface removal is less than $0.7\,mg/100\,cm^2$ glass

Table 5 – Chemical resistance of the obtained ceramic glazes in acidic and alkali solutions.

Sample	Acid resistance		Alkali resistance	
	Half loss in weight after 6 h mg/cm^2	Acid class	Loss in weight after 3 h mg/cm2	Alkali class
G5Z	1.4	2	41.7	1
G9Z	1.2	2	34.5	1
G13Z	0.64	1	21.2	1
G17Z	0.48	1	13.8	1

type is classified as class 1 highly acid resistance, above 0.7 up to 1.5 mg/100 cm^2 class 2 acid resistance, above 1.5 up to 15 mg/100 cm^2 slight acid attack and above 15 mg/100 cm^2 high acid attack [27]. Further, all studied ceramic glazes received class 1 chemical alkali resistance (solution, consisting of equal volumes of sodium hydroxide and sodium carbonate). According to DIN ISO 695 if the weight loss of the glass after 3 h of boiling is less than 75 mg/100 cm^2, the glass is alkali resistance class 1. Between 75 and 175 mg/cm^2 slight alkali attack, above 175 mg/cm^2 high alkali attack [28].

An improvement of the chemical resistance to acid attack (from class 3 to class 2) was achieved in the present study compared to our previous work when ZrSiO$_4$ was added as raw materials in glaze formulation [29]. It is known that the chemical resistance of ceramic glaze is related to its chemical composition and structure being a combination of the resistance of the glassy matrix, crystalline phases as well as the interfacial layer between them [30].

Depending on the properties as described above and exposure conditions (the type of solution, temperature, and time of exposure), the glaze surface can undergo ion exchange, dissolution or absorption reactions. Usually, ceramic glazes are resistant to acidic attack (excepting hydrofluoric acid) and alkalis attack. Alkali cations from the ceramic glaze network associated with less extent polymerized SiO$_4$ tetrahedral network are released to the acidic solutions by ion exchange with H$^+$ or H$_3$O$^+$ [29]. This reaction leads to the formation of a silica gel layer on the surface that acts as a barrier for further reactions. Furthermore, the alkali ions compensate for the negative charge such as AlO$_4^-$ and in this role are strongly bounded and cannot be easily detached during the corrosion process. The rate of the process is controlled by the diffusion rate of the ions, and decreases with time.

When the glaze surface is exposed to alkaline attack the dissolution of the glass network takes place by rupture of the Si—O bonds at a constant rate [31].

The substitution of SiO$_2$ by ZrO$_2$ improves the chemical resistance of the glaze and makes it less sensitive to changes in pH solution. Zirconia can take part in glaze structure as a network former or network modifier leading to an increase of bridging oxygen atoms per silicon and as a result ceramic glazes in the presence of Zr^{4+} will have a more packed structure and higher resistance [32].

Conclusions

In the present study, raw ceramic glazes with the addition of 5, 9, 13, 17 wt% ZrO$_2$, and 5 wt% of colemanite as a fluxing agent were prepared to evaluate zircon formation and its effect on glaze properties.

XRD, ^{29}Si MAS NMR, SEM-EDX, FTIR, and Raman Spectroscopy confirm the formation of ZrSiO$_4$ during the firing temperature of 1250 °C. XRD reveals an increase of ZrSiO$_4$ amount from 35 to 86 wt% with the increase of ZrO$_2$ content. Quantification of the relative intensity of zircon resonance in the ^{29}Si NMR spectra of ceramic glazes increases in the G5Z-G17Z series from 1.37 to 7.10%.

The chemical resistance results showed that the formation of ZrSiO$_4$ has a positive effect on the chemical resistance of the studied ceramic glazes.

The obtained results recommend the raw ceramic glazes prepared and investigated in the present study to be used as a cost-effective replacement to fritted compositions for ceramic substrates.

R E F E R E N C E S

[1] R. Pina-Zapardiel, A. Esteban-Cubillo, J.F. Bartolomé, C. Pecharromán, J.S. Moya, High wear resistance white ceramic glaze containing needle like zircon single crystals by the addition of sepiolite n-ZrO$_2$, J. Eur. Ceram. Soc. 33 (2013) 3379–3385, http://dx.doi.org/10.1016/j.jeurceramsoc.2013.05.033.

[2] M. Leśniak, W. Jastrzębski, M. Gajek, J. Partyka, D. Dorosz, M. Sitarz, The structure of model glasses of the amorphous phase of glass-ceramic glazes from the SiO$_2$–Al$_2$O$_3$–CaO–MgO–Na$_2$O–K$_2$O–ZnO system, J. Non-Cryst. Solid 515 (2019) 125–132, http://dx.doi.org/10.1016/j.jnoncrysol.2019.04.023.

[3] F. Güngör, H. Catır, M. Caki. Investigation of the microstructural changes of a number of glazes after they are applied and fired on two different bodies, Bol. Soc. Esp. Ceram. V. doi:10.1016/j.bsecv.2019.09.007.

[4] L. Froberg, T. Kronberg, S. Tornblom, L. Hupa, Chemical durability of glazed surfaces, J. Eur. Ceram. Soc. 27 (2007) 1811–1816, http://dx.doi.org/10.1016/j.jeurceramsoc.2006.04.162.

[5] M. Lusar, G. Monros, C.M. Rodrigues, J.A. Labrincha, Study of zircon or zirconia crystals addition in ceramic glazes by impedance spectroscopy, Ceram. Int. 31 (2005) 181–188, http://dx.doi.org/10.1016/j.ceramint.2004.04.003.

[6] R.J. Castilone, D. Sriram, W.M. Carty, R.L. Snyder, Crystallization of zircon in stoneware glazes, J. Am. Ceram. Soc. 82 (1999) 2819–2824, http://dx.doi.org/10.1111/j.1151-2916.1999.tb02162.x.

[7] G. Topateş, B. Alici, B. Tarhan, M. Tarhan, The effect of zircon particle size on the surface properties of sanitaryware glaze,

Mater. Res. Express 7 (2020) 015203, http://dx.doi.org/10.1088/2053-1591/ab657d.

[8] S. Wang, C. Peng, Z. Huang, J. Zhou, M. Lü, J. Wu, Clustering of zircon in raw glaze and its influence on optical properties of opaque glaze, J. Eur. Ceram. Soc. 34 (2014) 541–547, http://dx.doi.org/10.1016/j.jeurceramsoc.2013.08.018.

[9] N.V. Mazura, I.A. Levitskii, Use of colemanite for improving the quality of unfritted glazes, Glass Ceram. 65 (2008) 19–22, http://dx.doi.org/10.1007/s10717-008-9010-9.

[10] S. Akpinar, A. Evcin, Y. Ozdemir, Effect of calcined colemanite additions on properties of hard porcelain body, Ceram. Int. 43 (2017) 8364–8371, http://dx.doi.org/10.1016/j.ceramint.2017.3.178.

[11] B. Cicek, E. Karadaglia, F. Duman, Use of boron mining waste as an alternative to boric acid (H_3BO_3) in opaque frit production, Ceram. Int. 44 (2018) 14264–14280, http://dx.doi.org/10.1016/j.ceramint.2018.05.031.

[12] I. Atkinson, I. Teoreanu, M. Zaharescu, Characterization of multicomponent oxides system for glazes applications, Rev. Chim. 59 (2008) 990–993, http://dx.doi.org/10.37358/RC.08.9.1954.

[13] I. Atkinson, E.M. Anghel, C. Munteanu, M. Voicescu, M. Zaharescu, ZrO_2 influence on structure and properties of some alkali lime zinc aluminosilicate glass ceramics, Ceram. Int. 40 (2014) 7337–7344, http://dx.doi.org/10.1016/j.ceramint.2013.12.076.

[14] D. Massiot, F. Fayon, M. Capron, I. King, S.L. Calvé, B. Alonso, J.O. Durand, B. Bujoli, Z. Gan, G. Hoatson, Modelling one and twodimensional solid state NMR spectra, Magn. Reson. Chem. 40 (2002) 70–76, http://dx.doi.org/10.1002/mrc.984.

[15] I. Farnan, E.K.H. Salje, The degree and nature of radiation damage in zircon observed by ^{29}Si nuclear magnetic resonance, J. Appl. Phys. 89 (2001) 2084–2090, http://dx.doi.org/10.1063/1.1343523.

[16] K.J.D. MacKenzie, M.E. Smith, Multinuclear Solid State NMR of Inorganic Materials, Pergamon Press, Oxford, 2002.

[17] P. Dawson, M.M. Hargreave, G.R. Wilkinson, The vibrational spectrum of zircon ($ZrSiO_4$), J. Phys. C: Solid State Phys. 4 (1971) 240–256, http://dx.doi.org/10.1088/0022-3719/4/2/014.

[18] Z. Wang, Q. Xu, M. Xu, S. Wang, J. You, In situ spectroscopic studies of decomposition of ZrSiO4 during alkali fusion process using various hydroxides, RSC Adv. 5 (2015) 11658–11666, http://dx.doi.org/10.1039/c4ra12305k.

[19] V.G. Keramidas, W.B. White, Raman scattering study of the crystallization and phase transformations of ZrO_2, J. Am. Ceram. Soc. 57 (1974) 22–24, http://dx.doi.org/10.1111/j.1151-2916.1974.tb11355.x.

[20] S.M. Angel, N.R. Gomer, S.K. Sharma, K. McKay, Remote Raman spectroscopy for planetary exploration: a review, Appl. Spectrosc. 66 (2012) 137–150, http://dx.doi.org/10.1366/11-06535.

[21] E. Buixaderas, E.M. Anghe, S. Petrescu, P. Osiceanu, J. Solid State Chem. 183 (2010) 2227–2235, http://dx.doi.org/10.1016/j.jssc.2010.07.023.

[22] B.O. Mysen, D. Virgo, I. Kushiro, The structural role of aluminum in silicate melts – a Raman spectroscopics study at 1 atmosphere, Am. Mineral. 66 (1981) 678–701.

[23] A. Quintas, D. Caurant, O. Majerus, P. Loiseau, T. Charpentier, J.-L. Dussossoy, ZrO_2 addition in soda-lime aluminoborosilicate glasses containing rare earths: impact on the network structure, J. Alloys Compd. 714 (2017) 47–62, http://dx.doi.org/10.1016/j.jallcom.2017.04.182.

[24] F. Angeli, T. Charpentier, D. de Ligny, C. Cailleteau, Boron speciation in soda-lime borosilicate glasses containing zirconium, J. Am. Ceram. Soc. 93 (2010) 2693–2704, http://dx.doi.org/10.1111/j.1551-2916.2010.03771.x.

[25] S. Petrescu, M. Malki, M. Constantinescu, E.M. Anghel, I. Atkinson, R. State, M. Zaharescu, Vitreous and glass-ceramics materials in the SiO_2–Al_2O_3–MeO–M_2O type system, J. Optoelectron. Adv. Mater. 14 (2012) 603–612.

[26] O.C. Mocioiu, A.M. Mocioiu, A. Marin, M. Zaharescu, Study of historical lead silicate glasses and their preservation by silica coating, Ceram. Int. 43 (2017) 77–83, http://dx.doi.org/10.1016/j.ceramint.2016.09.055.

[27] DIN 12116:2001-03, Testing of glass – resistance to attack by a boiling aqueous solution of hydrochloric acid – method of test and classification.

[28] ISO695:1991-05, Glass-Resistance to attack by a boiling aqueous solution of mixed alkali: method of test and classification.

[29] I. Atkinson, M.E. Smith, M. Zaharescu, Examining correlations between composition, structure and properties in zircon-containing raw glazes, Ceram. Int. 38 (2012) 1827–1833, http://dx.doi.org/10.1016/j.ceramint.2011.10.007.

[30] T. Kronberg, L. Hupa, The impact of wollastonite and dolomite on chemical durability of matte fast-fired raw glazes, J. Eur. Ceram. Soc. 40 (2020) 3327–3337, http://dx.doi.org/10.1016/j.jeurceramsoc.2020.03.033.

[31] T. Kopar, V. Ducman, Low-vacuum SEM analyses of ceramic tiles with emphasis on glaze defects characterisation, Mater. Charact. 58 (2007) 1133–1137, http://dx.doi.org/10.1016/j.matchar.2007.04.022.

[32] F.M. Ezz-Eldin, V.M. Nageeb, Chemical resistance of some irradiated ceramic-glazes, Indian, J. Pure Appl. Phys. 39 (2001) 514–524.